ISSN 1027-5495. Functional Materials, 29, No.3 (2022), p. 429-436.
doi:https://doi.org/10.15407/fm29.02.429

Study of the effect of electromagnetic stirring on the quality of melt solidification in continuous casting

Yujun Li and Yihong Xu

School of Materials Science and Engineering, Jiujiang University, Jiujiang 332005, China

Received March 8, 2022

A heat transfer and solidification model based on the finite element method, validated by pin-shooting tests was created to predict the end-of-solidification state of various steel grades. Based on model and factory tests, favorable FEMS (Final Electromagnetic Stirring) modes have been determined, implemented for the best internal quality of bloom castings, in accordance with the solid fraction. The results show that the FEMS can play an obvious role in driving the residual melt and equiaxed grains in the direction of circular stirring if implemented correctly. It has been established that under optimal conditions for the implementation of FEMS, the central solid fraction should be in the range from 0 to 0.2 (^{0}C/^{0}C) to significantly improve the internal quality of the studied steel grades.

Keywords: implemented positions; FEMS (Final Electromagnetic Stirring); solid fraction; combination stirring; continuous casting bloom

Дослідження впливу електромагнітного перемішування на якість затвердіння розплаву за безперервного лиття. *Yujun Li and Yihong Xu*

Модель теплопередачі та затвердіння, заснована на методі кінцевих елементів, підтверджена випробуваннями з стрижнем голки, була створена для прогнозування стану кінцевого затвердіння різних марок сталі. На основі модельних та заводських випробувань були визначені умови реалізації електромагнітного впливу (FEMS) на розплав для кращої внутрішньої якості виливків блюмів у твердій фракції. Результати показують, що FEMS може відігравати важливу роль у русі залишкового розплаву та рівноосних зерен у напрямку кругового перемішування, якщо він коректно реалізований. Встановлено, що центральна тверда фракція в оптимальних умовах реалізації FEMS повинна бути в діапазоні від 0 до 0,2 (^{0}C/^{0}C), що доцільним для значного поліпшення внутрішньої якості марок сталі, що досліджуються.

1.Introduction

Electromagnetic Stirring (EMS) during bloom continuous casting is a key technique for improving the internal quality such as eliminating or reducing macrosegregation, porosity as well as shrinkage cavity. There are many variations of EMS methods according to their location on the strand, namely, in-mold stirring (MEMS), in-strand stirring (SEMS) using EMS under the mold, final mixing (FEMS) with EMS installation at the bottom of the secondary cooling zone end of the crater and combined mixing using at least two EMS [1-3].

It is well known that the effect of FEMS on reducing macrosegregation varies significantly depending on the coil current, mixing frequency and time or implemented positions. First of all, determining the location of the FEMS in the continuous casting bloom is the most important for obtaining the best metallurgical result. The implementation at too early or late stage of solidification cannot effectively improve the properties of the axial portion. When designing

Table 1. Chemical composition of steels, wt-%

Grade	C	Si	Mn	P	S	Cr	Mo	Ti	Al
20CrMnTi	0.20	0.20	0.90	0.018	0.008	1.13		0.06	0.025
42CrMoA	0.42	0.25	0.65	0.018	0.007	1.0	0.18		0.025
GCr15	1.0	0.25	0.35	0.018	0.007	1.50			0.020

a caster, the appropriate FEMS implementation conditions should been taken into consideration to match the casting process parameters such as casting speed, steel grades and strand section.

Based on the ingot tests, Mizukami et al. observed that the optimal moment for the implementation of FEMS should be immediately after the proportion of the solid is 0.1 in the center of the casting [4]. However, Oh and Chang indicated that the optimum thickness of the stirring pool at FEMS was determined to be 70, 54 and 30mm for the CC Blooms of P70, S82 and SU2 steel and 65 and 55mm for the S30 and S72 steel billets, respectively [5]. Sun et al. suggested that the optimal solidification ratio at the F-EMS for steel of GCr15, steel of 40Cr and steel of 50Mn were 72%, 68% and 75.05%, respectively [6]. In conclusion, there are three viewpoints about the favorable implementation conditions for FEMS as follows:

(1) The suitable implementation conditions for FEMS should be determined by the center solid fraction of 0.1.

(2) The optimum implementation conditions for FEMS should be determined by the solidification ratio ranged from 0.60 to 0.80.

(3) The favorable implementation conditions for FEMS should be based on the liquid pool thickness or the diameter of residual melt.

So far, the optimal conditions for the implementation of FEMS have not yet been clarified although the combined mixing method is widely used in many casters around the world. It follows from the previous study that the values of suitable liquid bath thickness, which determine the conditions for the implementation of FEMS, differ depending on the cross-sectional dimensions, and steel grades are less important for improving internal quality. The center solid fraction or the solidification ratio for the determination of the suitable conditions for the implementation of FEMS is still controversial. In particular, the FEMS implementation conditions are difficult to maintain at the 0.1 solids due to different continuous casting conditions. In addition, the performance of the FEMS is usually unsteady in steel plants due to confusion with the above concepts for the description of the solidification state of the strand crater end, especially, for steels with widely different solidification zone or mushy center state.

In the paper, a finite element model of heat transfer and solidification has been developed and validated by pin-shooting test [7] to predict temperature profile and solidification progress for a typical special steel bloom caster. Particular attention is paid to the identification of different states of final solidification for different steel grades with different solidification zones.

In the present work, one low-carbon special steel, one middle carbon special steel and one high carbon special steel, in which the defects of macrosegregation remain unsolvable in production, are adopted in a simulation analysis to optimize their FEMS practices. The main chemical difference between these steels is the carbon content, namely, C=0.20, 0.42 and 1.00% in 20CrMnTi steel, 42CrMoA steel and GCr15 steel, respectively, as shown in Table 1. The relationship between the center solid fraction and the solidification ratio is analyzed in order to determine the appropriate time points of the final rotational stirring in terms of solidification ratio or solid fraction at just before the crater end. According to the model, a series of plant trials were carried out with the same combination of EMC and different speeds using bloom caster Xining Special Steel Co.,Ltd. The effect of suitable FEMS implementation conditions on macrosegregation as well as chemical uniformity is evaluated.

2. Two Basic Concepts

The center solid fraction can be determined by the temperature at the center of the casting strand on the basis of the liquidus and solidus temperatures as follows:

$$f_{SC} = \frac{T_L - T_C}{T_L - T_S} \quad (1)$$

where T_L and T_S are liquidus temperature and solidus temperature, respectively. T_C is the temperature in the center of the casting.

As we know, theoretically, the value of the central solid fraction, which is related to the central temperature and solidification state in the solid-liquid coexistence zone or the mushy zone, should be a positive number between zero and one. To describe possible widely differing core temperatures or solidification states, a negative core solids value less than 0 is allowed in the article. Thus, in the description of the strand center, $f_{SC} < 0$ refers to the entire liquid zone even with superheat, $0 < f_{SC} < 1$ refers to the mushy zone of coexistence of solid and liquid phases, and $f_{SC} = 1$ refers to the completely solidified zone even with temperature under T_s.

The solidification ratio is estimated by the following equation:

$$D_{DS} = \frac{A}{A_0} \tag{2}$$

where, A_0 and A denote the strand cross section area and the solidified shell area in the cross section, respectively.

If we combine equations (1) and (2), there is a case $f_{SC}=D_S=1$, when the strand is fully solidified.

3. Heat Transfer and Solidification Model

3.1 Model description

The heat transfer and solidification model is obtained on the basis of the following assumptions [8]:

(1) The heat transfer in the casting direction is relatively small enough and negligible.

(2) The suitable effective thermal conductivity is set to compensate the effect of molten steel flow or convection in the strand liquid pool and mushy zone on transfer heat.

(3) In the secondary cooling spray zones, the appropriate cooling rate is assumed to be the same for each zone, where the cumulative heat transfer coefficient is used to describe the total surface heat transfer, including radiation, roller contact, and air mist convection heat transfer. In order to achieve a precise prediction of the temperature field and solidification behavior in the bloom casting process, the two-dimensional unsteady state conduction equation is used [9]:

$$\rho C_{eff}\frac{\partial T}{\partial t} = \frac{\partial}{\partial X}\left(k\frac{\partial T}{\partial x}\right) + \frac{\partial}{\partial y}\left(k\frac{\partial T}{\partial y}\right) \tag{3}$$

where ρ is the density, C_{eff} is the effective specific heat, x and y are the coordinate directions along width and along thickness, respectively, and k is the thermal conductivity of steels depending on temperature.

The initial and boundary conditions for the solution of Eqs.(3) are expressed as follows:

$$t = 0, \quad 0 \le x \le \frac{W}{2}, \quad 0 \le y \le \frac{Th}{2}, \quad T = T_M \tag{4}$$

$$t \ge 0, \quad x = \frac{W}{2}, \quad -k\frac{\partial T}{\partial x} = 0 \tag{5}$$

$$t \ge 0, \quad y = \frac{Th}{2}, \quad -k\frac{\partial T}{\partial y} = 0 \tag{6}$$

$$t > 0, x = 0, \quad -k\frac{\partial T}{\partial x} = q_{0x} \tag{7}$$

$$t > 0, y = 0, \quad -k\frac{\partial T}{\partial y} = q_{0y} \tag{8}$$

where W and Th are the width and thickness of strand, respectively, T_M is the casting temperature, qo is the surface heat flux.

The centerline boundary conditions (at $x = W/2$ and $y = Th/2$) assume that the heat flux at the centerlines of the casting is symmetrical; therefore, only one quarter section of the casting needs to be considered. The outside heat flux around the perimeter of the bloom is assumed to be constant, so that q_{ox} is equal to q_{oy}. The surface heat flux term is characterized in each of the three cooling zones and can be obtained as:

Mold zone:

$$q_0 = 2680000 - b\sqrt{\frac{L}{\upsilon}} \tag{9}$$

where,

$$b = \frac{1.5\times(268000 - \overline{q})}{\sqrt{\frac{L_m}{\upsilon}}} \tag{10}$$

$$\overline{q} = \frac{C_w \times m \times \Delta T}{S_{eff}} \tag{11}$$

where L and L_m are the local distance to the meniscus and the effective length of the mold, respectively; υ is the casting speed; $\overline{q}$ is the average heat flux in the mold zone; C_w is the specific heat of water; m is the

Table 2. Comparison of the shell thicknesses by the model calculations and pin-shooting tests

Sample number	Steel grade	Casting speed, m/min	Distance from meniscus, m	Shell thickness by pin-shooting, mm	Shell thickness by the model, mm	Error,%
1	20CrMnTi	0.4	18.25	202	203.4	0.69%
2	42CrMoA	0.4	18.25	185	183.5	-0.82%
3	GCr15	0.4	18.25	159	158.2	-0.50%
Averaged						0.67%

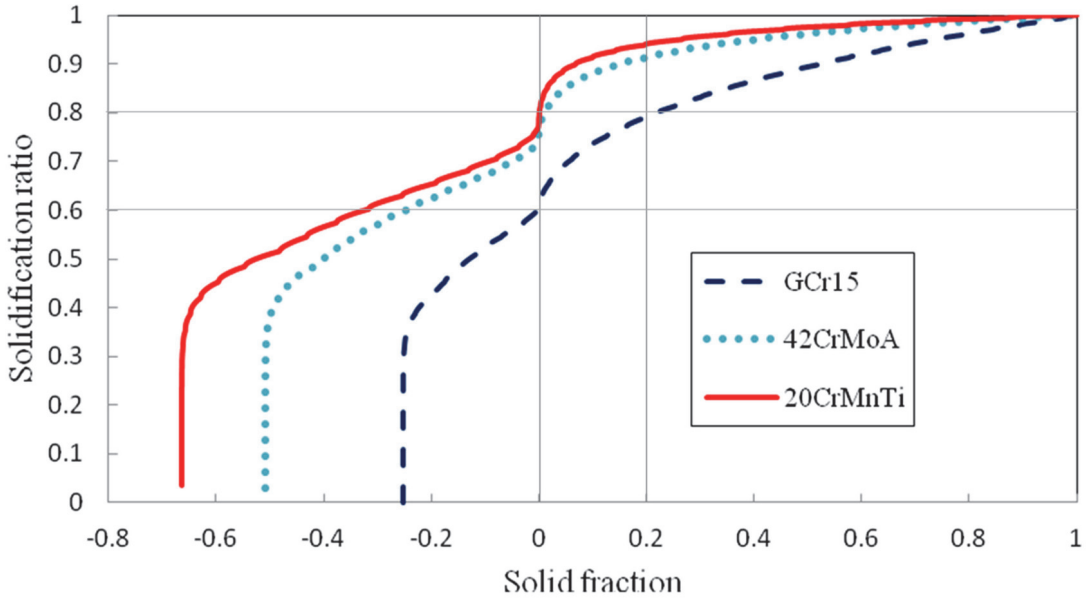

Figure 1. Relationship between center solid fraction and solidification ratio

water flow rate for cooling of the mold; ΔT is the temperature difference of the mold cooling water, and S_{eff} is the active area of the mold.

Spray zone:

$$q_0 = h_S(T_0 - T_{ws}) \tag{12}$$

Here T_0 and T_{ws} are the local surface temperature of the strand and the temperature of cooling water, respectively; and h_s is the integrated heat transfer coefficient at the strand surface, which can be estimated by:

Water spray region,

$$q_0 = h_S(T_0 - T_{ws}) \tag{13}$$

Air-mist spray region [10],

$$h_S = 116 + 10.44w^{0.851} \tag{14}$$

where w is the secondary cooling water flow rate.

Radiation zone:

$$q_0 = \sigma K(T_0^4 - T_a^4) \tag{15}$$

where T_{a} is the ambient temperature, σ is the blackness, and K is Boltzmann's constant.

3.2 Model validation by Pin-shooting

Pin-shooting tests are carried out to calibrate and validate the model of heat transfer and solidification for the given typical steel grades, namely, steel of 20CrMnTi, steel of 42CrMoA and steel of GCr15, through the narrow surface of the strand. Table 2 shows the final solidified shell thicknesses calculated by the model and those obtained by pin-shooting tests.

As seen in Table 2, the shell thicknesses calculated by the modified model are finally agreeable well with those obtained by pin-shooting tests with relative error less than 1%, and thus, the model can accurately describe the solidified shell thickness for the given steel grades during casting. Accordingly, the solidification ratio and the center solid fraction of the castings can be precisely estimated in the solidification process.

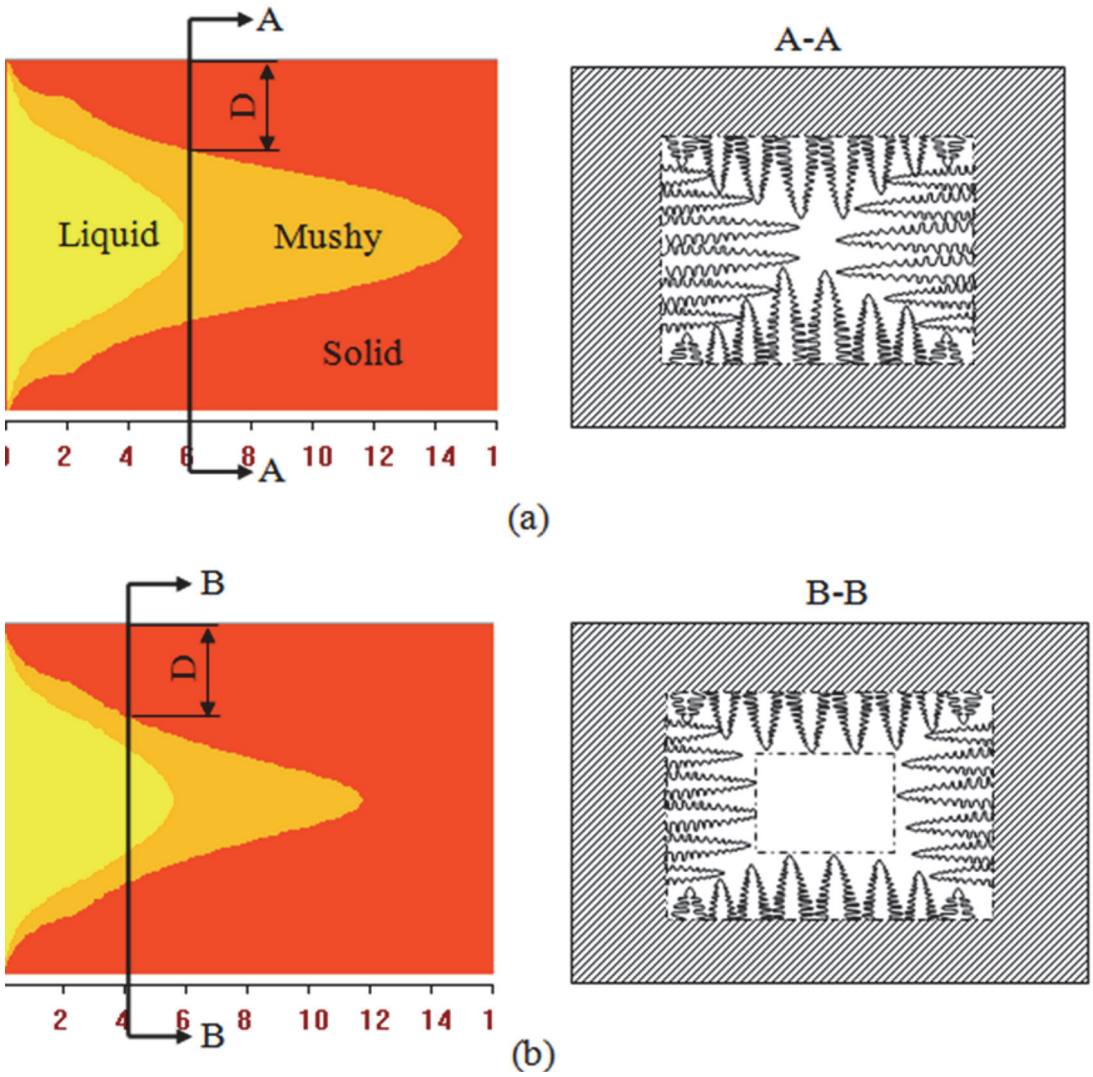

Figure 2. Schematic diagram of solidification process and center solidification state for (a) high carbon steels and (b) low carbon steels at the same solidification ratio

3.3 Center solid fraction and solidification ratio

The relationship between central solids (f_{SC}) and solidification degree (DS) of steel grades was calculated for 410 mm × 530 mm bloom casting processes with the same casting speed of 0.43 m/min, superheat degree of 30K, specific water consumption of 0.13 l/kg, as shown in Figure 1.

It is shown that, under the same condition of the center solid fraction, the solidification ratio of GCr15steel is less than that of 42CrMoA steel and both less than that of 20CrMnTi steel. In other words, with the same central solid fraction, the solidification ratio decreases with increasing carbon content in the steel. On the other hand, at a certain solidification ratio, the solid fraction of GCr15 steel is higher than that of 42CrMoA steel, and both are higher than that of 20CrMnTi steel. Accordingly, for a given solidification ratio, the center solid fraction increases with increasing carbon content in steel.

According to the above definition, the solidification ratios ranged from 0.60 to 0.80 correspond to the range of the solid fractions for the three steel grades as following: 0 to 0.20 for GCr15 steel, where there is a mushy liquid-solid state in the bloom centerline region; -0.25 to 0.01 for 42CrMoA steel, where there is a transition zone of coexistence of pure liquid and liquid-solid states; and -0.32 to 0 for 20CrMnTi steel, where a complete pure liquid exists in the centerline region. Accordingly, for given center solid fractions ranged from 0 to 0.20, the local solidification ratios of the bloom strand for the three

Table 3. Main process parameters of continuous casting machine

Parameters	Values	Units
Caster type	Curved	
Sectional dimensions	410×530	mm^2
EMS	MEMS+FEMS	
Casting Speed	0.32~0.5	m/min
Caster radius	16.5	m
Mould length	780	mm
Pouring mode	Submerged	
Secondary cooling zone	Four segments	
Secondary cooling zone length	0.35+1.8+2.2+3.5	m

different steels are 0.60 to 0.80 for GC15; 0.75 to 0.91 for 42CrMoA, and 0.78 to 0.94 for 20CrMnTi, respectively. For this reason, while for GCr15 high carbon steel, a solidification ratio in the range of 0.6 to 0.8 is assumed at the exact positions realized by FEMS in the central mushy zone, for 20CrMnTi steel, however, it is actually a kind of SEMS due to its pure liquid state along the centerline corresponding to the specified solidification ratios.

Thus, the implementation of FEMS is suitable for solid fractions in the range of solidification ratios from 0 to 0.20 for all steel grades, and with crystallization factors from 0.60 to 0.80 it is suitable only for high carbon steels.

For a given local solidification at a solid-to-liquid ratio of 0.60 for both high carbon and low carbon steel, the strand solidification progress and the solidification state in cross section are shown in Figure 2. It is clear that for a given solidification ratio of the strand in the central region there is a very different state of solidification. Therefore, the center solid fraction ranged from 0 to 0.2 should be recommended as a criterion for suitable FEMS implementation positions, which is applicable for all steel grades.

4. Industry Experiment

Plant trials on the suitable FEMS implementation positions of bloom casting for various steels have been carried out in the No.2 caster of Xining Special Steel. In the experiments, the center solid fraction at the

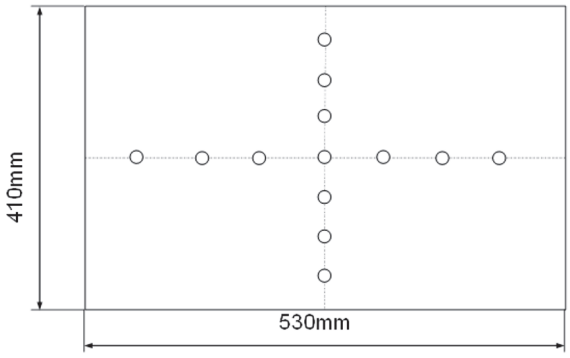

Figure3. Sampling schematic for wet chemical analysis in bloom cross sections

location of FEMS is varied mainly by controlling casting speed at a suitable super heat and specific water flow rate. The main process parameters of the continuous casting machine are briefly listed in Table 3. Table 4 gives the major specifications of the combination EMS. Schemes of FEMS for the bloom casting are shown in Table 5.

To evaluate the macrosegregation in the bloom cross section, chemical analysis of carbon was carried out. The samples 5mm in length and 5.5 mm in diameter are taken by drilling through the cross section of the bloom as shown in Figure 3.

The center carbon segregation index N is obtained based on the carbon analysis of a sample as follows:

$$N = \frac{nC_0}{\sum_{i=1}^{n} C_i} \tag{16}$$

where C_0, C_i and n denote the central carbon content, the local carbon content and the number of the carbon content C_i as shown in Figure 3, respectively.

5. Results and Discussion

The macrograph of the etched cross section is shown in the Figure 4. In the figure, distinct radial streaks are observed in a core zone where fine grained equiaxed crystals are accumulated as a result of strong stirring. It is supposed that the remained streak is formed in the mushy zone due to the final electrical magnetic stirring; this means that the FEMS plays a dominant role in driving the residual melt and equiaxed crystals in the direction of circular stirring.

Table 4. Major specifications of EMS in the bloom caster

Parameters	M-EMS	F-EMS
Current, A	Low/middle carbon steel:700; High carbon steel:820	Low carbon steel:580; Middle carbon steel:660; High carbon steel:700
Frequency, Hz	1.5	7.5
Rotation direction	Constant	Constant
Installed location of EMS (distance from meniscus), m	0.55	16

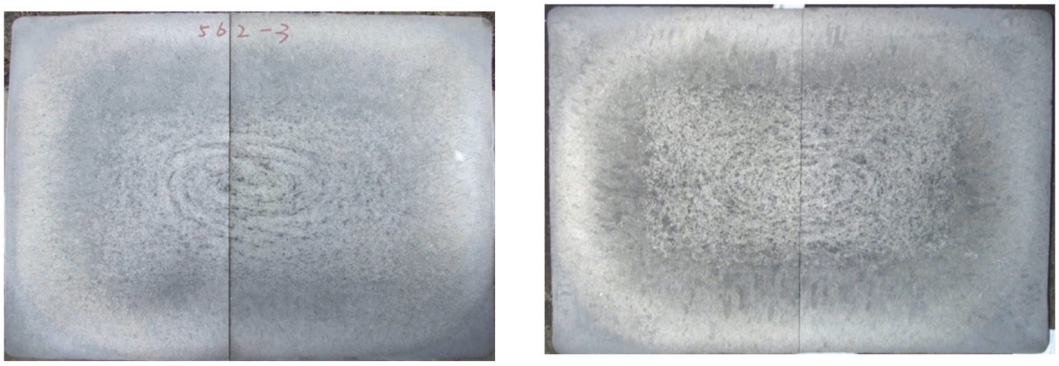

(a)42CrMoA (b)20CrMnTi

Figure 4. Macrograph of etched sections of bloom castings with FEMS: (a) 20CrMnTi steel (segregation index N = 1.03); (b) 42CrMoA steel (segregation index N = 1.01)

The center segregation indices (N) are 1.03 and 1.01 for 20CrMnTi and 40CrMoA steels, respectively. It is shown that a satisfactory metallurgical effect of FEMS has been obtained for both the steels.

Figure 5 shows the local flow field in the central cross sections obtained using a coupled electromagnetic flow dynamic model that assumes different melt viscosity for two types of steels due to the different proportion of solids at the center. The maximum flow velocities of the center melt of 42CrMoA and 20CrMoA steels driven by electromagnetic force are 0.13m/s and 0.18m/s, respectively. According to H. Mizukami et al. [4], a casting without segregation can be obtained when the FEMS stirring velocity in the center melt is kept in the range of 0.10 m/s to 0.20m/s. Accordingly, the stirring times or implementation positions should be favorable for the bloom casting with a center solid fraction in the range of 0.03 to 0.16.

As shown in Table 4, the solidification ratios in the two schemes are 0.92 and 0.83, respectively, which are not in the popular recommended range from 0.60 to 0.80. The center solid fractions, however, are 0.16 and 0.03, respectively, which are both in the recommended range from 0 to 0.20. Thus, it has been proven that a central solid fraction ranging from 0 to 0.2 for various steels is a reliable criterion for suitable FEMS implementation positions that can be expected to eliminate or reduce center line segregation.

Table 5. Schemes of FEMS for bloom continuous casting

Type	Steel grades	Casting speed, m/min	Super heat, K	Specific water flow rate, L/kg	Solidification ratio, m^2/m^2	Solid fraction, $^{O}C/^{O}C$
A	20CrMnTi	0.37	39	0.16	0.92	0.16
B	42CrMoA	0.40	35	0.15	0.83	0.03

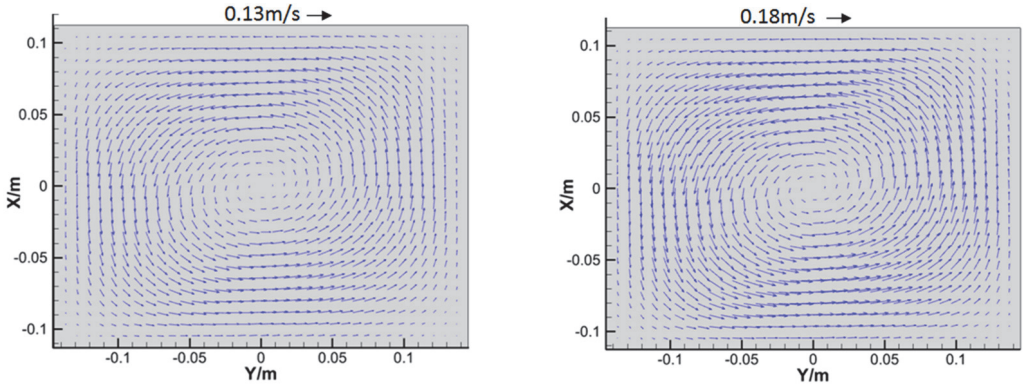

(a)42CrMoA (b)20CrMnTi

Figure 5. Flow fields in the bloom cross sections at given center solid fractions

6. Conclusion

Based on the finite element heat transfer and solidification model and plant trials, the reasonable FEMS implementation positions for better internal quality of bloom castings have been determined according to solid fraction. The main conclusions are summarized as follows:

1.The much different center solid fractions for various steel grades have been found at a given strand solidification ratio and vice versa.

2.The criterion of the effective FEMS implementation positions based on the solidification ratio with a solid-to-liquid ratio ranged from 0.6 to 0.8 has been proved to be suitable only for high-carbon steels or with a longer solidification zone.

3.A suitable central solid fraction in the range of 0 to 0.2 is recommended for all steels as a criterion for the FEMS implementation position at which an increase in internal quality can be expected.

References

1. T.Wang, L.Zhang, H.Wu, X.Zhang, *Processes*, **10**, 430(2022).
2. Q.P.Dong, J.M. Zhang, Y.B.Yin, H. Nagaumi, *Journal of Iron and Steel Research International*, **29**, 612 (2022).
3. H.Xiao, P.Wang, B.Yi, X.Chen, A.Li, H.Tang, W.Li, *J. Zhang, Metals* , **11**, 6(2021).
4. H.Mizukami, M.Komatsu, T.Kitagawa, K.Kawakami, *Transactions of the Iron and Steel Institute of Japan*, **24**, 923(1984).
5. K. S.Oh, Y. W.Chang, *ISIJ International*, **35**, 866 (1995).
6. H. Sun, L. Li, X. Cheng, W.Qiu, Z.Liu, L.Zeng, *Ironmaking and Steelmaking*, **42**, 439 (2015).
7. T. Kawawa, H. Sato, S. Miyahara, T. Koyano, H.Nemoto, *Tetsu-to-Hagane* , **60**, 206 (1974).
8. H.Sun, J. Zhang, *Metallurgical and Materials Transactions B*, **45**, 1133(2014).
9. Y. Meng, B. G. Thomas, *Metallurgical and Materials Transactions B*, **34**, 685 (2003).
10. J. K.Brimacombe, *Canadian Metallurgical Quarterly*, **15**, 163 (1976).